VAGINAL MUCOSAL IMMUNITY BASED ON IgG-MUCIN CROSSLINKING

Arthi Kannan

A thesis submitted to the faculty of the University of North Carolina at Chapel Hill in partial fulfillment of the requirements for the degree of Master in the Department of Biomedical Engineering

Chapel Hill
2013

Approved by:

Samuel Lai

Ronald Swanstrom

Brian Button

ABSTRACT

Arthi Kannan: Vaginal Mucosal Immunity Based on IgG- Mucin Crosslinking
(Under the direction of Samuel Lai)

In this thesis, I investigated whether IgG, the predominant antibody in cervicovaginal mucus (CVM), can interact with CVM constituents to protect against Herpes Simplex Virus 1 (HSV-1) infection. Despite the weak affinity between individual IgG molecules and mucins, we hypothesize that multiple virion-bound IgG can avidly crosslink HSV-1 to the mucin mesh, thereby preventing HSV-1 from reaching the target cells. Consistent with this hypothesis, I showed that HSV-1 freely diffused through pH-neutralized CVM with low levels of anti-HSV-1 IgG, but was immobilized in samples with modest levels of endogenous or exogenously added anti-HSV-1 IgG. Removal of the Fc domain and N-glycans from IgG both markedly reduced its trapping potency. Finally, a non-neutralizing monoclonal IgG against HSV-gG provided significant protection against vaginal HSV challenges in mice, and this protection was eliminated in the absence of mucus. These results strongly suggest secreted IgG can work in tandem with mucus to block infections.

ACKNOWLEDGEMENTS

First and foremost, I would like to thank my PI, Dr. Samuel Lai, without whom this project would not have been possible. He has been a great inspiration and a wonderful support throughout this journey and I really am glad that I got to work with him and in his lab. I would also like to thank Dr. Ron Swanstrom, and Dr. Brain Button, my thesis readers, for graciously agreeing to be on my thesis committee.

Without the support and guidance of my family and friends, I wouldn't be who I am today, so I am very grateful to them. Last but definitely not the least, I would like to give my appreciation to my fellow lab mates, who made this journey as enjoyable as possible and for providing a great work setting. A special thanks to Ying-Ying, Kenetta, Mike and Babu, all of whom made valuable contributions to this project.

TABLE OF CONTENTS

LIST OF TABLES

LIST OF FIGURES

CHAPTER 1

INTRODUCTION

1.1 Mucus as a protective barrier

Mucus is a viscous and elastic gel that coats any exposed surface not covered by skin, including the respiratory, gastrointestinal and urogenital tracts. In addition to enabling many essential processes in life such as blinking, swallowing and copulation, mucus is generally thought to serve as the first line of defense against pathogens and infections. Indeed, mucus serves as a selectively permeable barrier allowing entry of nutrients while regulating the entry of foreign and dangerous substances, although the mechanisms are not well understood. (Cone, 1999)

The major constituent of mucus gel is mucins, long glycoproteins secreted by globlet cells. Mucin is the most abundant biopolymer produced in the body. In addition, many constituents are secreted into mucus such as antibodies, protective factors, different types of mucins, ions, lipids, proteins and water. (Cone, 1999) Mucus is constantly secreted and renewed; this constant shedding ensures that particles trapped in mucus gel are quickly eliminated from a mucosal surface. The composition of mucus and the mucosal environment are constantly changing to ensure the proper mucus function. For example, the secretion of pathogen specific antibody is dependent upon the presence of the specific pathogens. “Thus the protective functions of mucus are dynamic processes, depending on relative rates of outward secretion and ward diffusion, and on the relative rates of mucus shedding and microbial growth.” (Cone, 1999)

1.2 Viscoelasticity of mucus

The viscoelastic property of mucus gel is what enables it to act as a selectively permeable barrier as well as a lubricant. At the macro level, mucus behaves as a non-newtonian fluid and possesses both substantial viscous and elastic properties under little to no shearing. This unique mechanical characteristic is derived from a dense mesh network of mucin fibers, which are crosslinked and entangled to form a gel. The interactions between mucin fibers ensures mucus behaves as a gel under low shear conditions, but readily shear thins and functions as a lubricant when subjected to large and rapid shear forces. (Lai et al., 2009 and Cone 1999). Also, the glycosylated mucin fibers are enriched with sulfate and sialic acid groups, leading to a net negative charge which increases mucin rigidity and high sialomucin leads to high viscosity. (Lai et al., 2009) The viscoelasticity of mucus is delicately balanced such that mucus gel is not too viscoelastic to be transported and removed from a mucosal surface while still maintaining sufficient adhesive and elastic strength to associate to epithelial surfaces and immobilize pathogens.

Improper balance of the viscoelasticity of the mucus can lead to altered physical properties of mucus and consequently to different disease conditions. Furthermore, the biochemical environment of mucus can change due to person's age, diet, presence of specific antigens, commensals and pathogens. For example, one such disease state is bacterial vaginosis (BV), where there is an overgrowth of polymicrobes and a decrease of commensal lactobacilli. The overgrowth of BV bacteria helps break down the mucus gel because these bacteria produce sialidase and other enzymes that degrade the mucins which reduces the viscoelasticity of mucus. (Lai et al., 2009 and Cone 1999) The alteration in the vaginal microflora leads to increased risk for acquiring varies STDs in patients that have BV since it is unlikely degraded mucins will

possess sufficient viscoelasticity to effectively trap pathogens. In the female reproductive tract, cervicovaginal mucus secretions are also known to be markedly altered by the menstrual cycle. During ovulation, the viscoelasticity of cervical mucus decreases, allowing sperm to swim through freely and possibly reaching the upper reproductive tract. During, non-ovulatory phase, the increased viscoelasticity of mucus makes it much more difficult for sperm to swim through. (Cone, 1999)

Changes in mucus clearance and secretion rates can also substantially alter the mucus barrier. For example, rapid mucus clearance ensures that trapped pathogens are quickly eliminated. Constant mucus secretion also ensures that pathogens must travel upstream against the mucus current to reach the epithelium, and this leads to a greater transit time. The greater transit time in turn allows more pathogens to become inactivated, degraded or eliminated before reaching target cells. (Cole, 2006 and Cone, 1999)

1.3 Secreted antibodies in mucus

There are more antibodies secreted into mucosal secretions than into the blood or lymph. The secretions of mucosal antibodies are regulated by M cells, which are dispersed periodically across mucosal surfaces. Because the regions around the cells are not coated by mucus, any particles/pathogens that are not trapped by mucus are often directed to and become internalized by the M cells. Thus, M cells function as sensory checkpoints for the cellular immune system, and leads to B cell expansion and secretion of antigen-specific antibodies. (Cone, 1999) Secreted antibodies themselves likely play an important role in protecting us against the pathogens. Antibodies can block receptor binding sites (i.e. neutralize), or trigger different effector functions such as opsonization, antibody-dependent cell-mediated cytotoxicity (ADCC) and complement activation, and agglutination of pathogens. In mucus from a healthy vagina, these effector

functions are typically very limited due to a scarcity of live immune cells and little complement activity (Cone, 1999; Hill and Anderson, 1992; Schumacher, 1988). Our inadequate understanding of vaginal immunity was recently highlighted by the Thai HIV (RV144) vaccine trial that showed confounding results where significant protection was observed with non-neutralizing antibodies. (Kresge, 2009; Rerks-Ngarm et al., 2009) Vaccinated subjects showed reduced risk of HIV acquisition, but little to no systemic protection (e.g. reduction in serum titers) once an infection was acquired. This implies that vaccine-elicited antibodies were able to provide protection before the initiation of infection, but did not neutralize or elicit other effector functions. These results served as a major impetus in my search for alternative mechanisms of vaginal immunity.

In this thesis, I explored whether secreted antibodies can work together with mucus to facilitate protection against infectious pathogens that are transmitted across the mucosal surface. The hypothesis that formed the basis of my work, originally proposed by Richard Cone nearly 20 years ago, is that secreted antibody can interact with mucus to permanently crosslink pathogens to the mucus gel, thereby preventing the entry of infectious pathogens to the target epithelium. Viruses, such as HSV and HPV, can freely diffuse through mucus (Olmsted et al., 2001 and Lai et al., 2009a). Thus the slightly retarded diffusivities of antibodies in mucus by 10% compared to saline suggest the antibodies can form weak, transient interactions with the mucus gel, rather than steric hindrance since virus particles much larger than IgG are able to readily diffuse through as can be seen from Figure 1.1 (Olmsted et al., 2001). Likewise, removal of 10 Fab domains in IgM did not alter the measured IgM-mucin affinity, suggesting that the Fab domain is unlikely to play a role in the interaction (Olmsted et al., 2001). The short lived affinity bonds still lets antibody to diffuse outward and attach to the pathogens that are entering the mucus

secretions. Although, individual antibodies are hardly slowed, multiple of antibody can bind to the same pathogen at once, and in turn confer multiple low-affinity antibody-mucin crosslinks to the same pathogen. This should immobilize the pathogen to the mucus gel with high avidity. Trapping in mucus directly reduces the flux of viruses reaching target cells, and constant shedding/clearance and other protective factors in mucus will quickly eliminate or inactivate the infectious pathogen. (Cole, 2006; Doss et al., 2010)

1.4 Importance of the antibody-mediated trapping mechanism

Many studies on mucosally transmitted infections to date had largely ignored the role of mucus. I believe that if we can better understand how the immune system can work together with mucus to protect, it is possible to better harness this protective mechanism to develop improved methods for reinforcing the first line of defense against various sexually-transmitted infections, including HIV, HSV, HPV and bacterial infections. This includes developing vaccines with a specific and desired mucosal response profile. Likewise, we can engineer new generations of topical prophylaxis monoclonal antibodies for mucus surfaces.

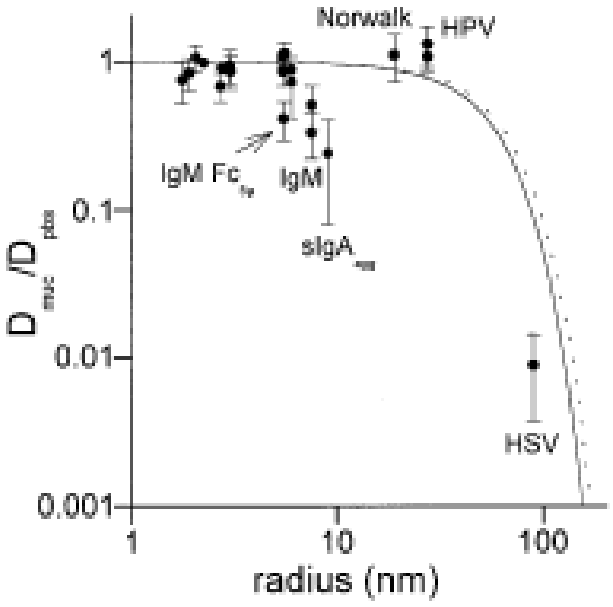

Figure 1.1: Normalized diffusion coefficients for proteins and viruses in mucus.

***D*muc/*D*pbs ± SD is plotted for different particles.** If a particle diffuses in mucus as fast as it diffuses in saline, *D*muc/*D*pbs =1. (Figure from Olmsted et al., 2001)

CHAPTER 2

IgG FC-MUCUS INTERACTIONS PREVENT INFECTIONS BY TRAPPING VIRUSES IN MUCUS[1]

2.1 INTRODUCTION

Large quantities of IgG are transported into female genital tract mucus secretions by the MHC class I-related neonatal Fc receptor (Li et al., 2011), resulting in at least ten-fold more IgG than IgA (Usala et al., 1989). However, despite this predominance of IgG, surprisingly little is known about the roles that secreted IgG may play in preventing mucosal infections. Vaginal protection against viral infection does not necessarily require IgG-mediated neutralization; robust protection was observed with IgG against HIV-1/SIV topically applied to the rhesus macaque vagina even at sub-neutralizing concentrations or with poor neutralizing activity (Mascola et al., 2000). In addition, well-studied antibody (Ab) effector functions in the blood and lymph (e.g., complement activation, antibody-dependent cell-mediated cytotoxicity (ADCC)) are absent or limited in healthy female genital secretions, which typically have little complement activity and few if any active leukocytes (Cone, 1999; Hill and Anderson, 1992; Schumacher, 1988). These classical mechanisms of systemic immune protection also do not adequately account for the moderate but significant protection observed in the landmark Thai RV144 HIV vaccine trial

[1] This chapter is a manuscript that has been submitted for publication and I am the first co-author on the paper. I was involved in experimental design, data analysis/discussion and writing of the manuscript. Also, I carried out the follow experimental procedures for the paper : culturing and purification of fluorescent HSV-1, preparation and characterization of anti-HSV-1 IgG, anti-HSV-1 F(ab)'2, and deglycosylated anti-HSV-1 IgG, assisted with neutralization assay, multiple particle tracking of HSV-1 in CVM and characterized the anti-HSV-1 gG used in mouse studies.

(Kresge, 2009; Rerks-Ngarm et al., 2009). The vaccination regimen modestly reduced the risk of HIV acquisition despite inducing primarily non-neutralizing Ab and otherwise offering little to no protection against systemic progression of infections once acquired, suggesting that protection likely occurred *prior* to initiation of infection.

To reconcile these observations, we propose that secreted IgG may have evolved to work *in tandem* with mucus to trap and thereby exclude individual pathogens (Cone, 1999). Viruses must penetrate CVM to reach and infect their target cells in the vaginal epithelium; indeed, we have shown that HIV and human papillomavirus (HPV) are both capable of rapidly diffusing through human genital mucus secretions (Lai et al., 2009a; Olmsted et al., 2001). We also previously found that the diffusion of IgG (11 nm) was slowed slightly in human cervical mucus compared to saline buffer, while much larger virus-like particles, including the capsids of Norovirus (38 nm) and HPV (55 nm), were not slowed by this mucus (Olmsted et al., 2001). Thus, the slight retardation of the much smaller IgG molecules must be due to very transient (< 1 s), low-affinity bonds with the mucin mesh (Olmsted et al., 2001). These observations prompt our hypothesis that, by making only transient low-affinity bonds with mucins, IgG is able to diffuse rapidly through mucus and accumulate on a pathogen surface. The array of pathogen-bound Ab in turn can effectively trap the pathogen in mucus gel by ensuring at least some low-affinity bonds to the mucin mesh are present at any given time (Fig. 2.1). Virions trapped in CVM cannot reach their target cells, and will instead be shed with post-coital discharge and/or inactivated by spontaneous thermal degradation as well as additional protective factors in mucus, such as defensins (Cole, 2006; Doss et al., 2010).

2.2 RESULTS AND DISCUSSION

We chose to explore this trapping-in-mucus hypothesis using HSV-1 (d ~180 nm), a highly prevalent sexually transmitted virus. We collected fresh, undiluted CVM obtained predominantly from donors with normal lactobacillus-dominated vaginal microbiota, as confirmed by Nugent scoring (Table 2.1). HSV-1 virions expressing a VP22-GFP tegument protein construct, packaged into virions at high copy numbers while maintaining native viral envelope integrity, were mixed into CVM pH-neutralized to mimic neutralization by alkaline seminal fluid. We then performed time-lapse microscopy of virion motions in real-time with high spatiotemporal resolution (15 fps; 10 nm tracking resolution), and quantified virion mobility using multiple particle tracking over a long time scale. We observed substantial differences in HSV-1 mobility in CVM samples from different donors (Fig. 2.2 A): in 7 of 12 CVM samples, most virions diffused distances spanning several microns over the course of 20 s, whereas in the remaining 5 CVM samples, the majority of virions were essentially trapped, moving less than their diameter (<200 nm) in 20 s.

Since IgG is the predominant immunoglobulin in human CVM (Usala et al., 1989), we examined whether virion mobility correlated with endogenous virus-specific IgG in all 12 CVM samples using a whole-virus ELISA assay (Table 2.2). In good agreement with our hypothesis, HSV-1 diffused rapidly through all CVM samples that had little or no detectable endogenous anti-HSV-1 IgG (< 0.2 μg/mL; detection limit 0.017 μg/mL) at rates only several-fold lower than their expected rates in water (Fig. 2.2). In contrast, in samples with elevated levels of endogenous anti-HSV-1 IgG (≥ 0.6 μg/mL), most HSV-1 virions were effectively trapped. HSV-1 trapped over the course of 20 s remained trapped in the same locations for at least 15 min (data not shown). In the same CVM samples, control latex nanoparticles comparable in size to HSV-1 and engineered with muco-inert coatings (PS-PEG; d ~200 nm) exhibited rapid diffusion (data not shown), in good agreement with our previous observations of the large pores

present in human CVM (average ~340 nm) (Lai et al., 2007; Lai et al., 2010). Thus, the mucus mesh spacing was large enough for IgG-coated HSV-1 (at most 15-20 nm larger diameter even at saturation) to diffuse relatively unimpeded in the absence of adhesive interactions with mucin gel. Muco-adhesive latex nanoparticles of the same size (PS; d ~200 nm) were markedly slowed or immobilized in the same CVM secretions (data not shown). Importantly, observations with PS-PEG and PS control particles confirmed that the general barrier properties of all samples, including those with low levels of endogenous anti-HSV-1 IgG, remained intact. After removal of ~90-95% of total IgG from these samples by dialysis at constant sample volume, HSV-1 became readily mobile (Video S3), whereas PS beads remained immobilized (data not shown). HSV-1 mobility did not correlate with total IgG, IgA or IgM content only with HSV-1 specific IgG.

A well-recognized mechanism of mucosal immune defense is 'immune exclusion' in which microorganisms in the gut are agglutinated by secreted polyvalent IgA and IgM into clusters too large to diffuse through mucus (Hamburger et al., 2006; Mantis et al., 2011). However, we observed little to no agglutinated HSV-1 in our experiments, consistent with previous findings that IgG is a relatively poor agglutinator (Berzofsky et al., 1993). Together, these observations suggest that individual HSV-1 virions in samples with elevated endogenous levels of anti-HSV-1 IgG are slowed by multiple low-affinity bonds with CVM rather than by physical (steric) obstruction.

To confirm that trapping of HSV-1 in CVM was mediated specifically by IgG bound to virions and not by any other component in mucus that might be associated with elevated endogenous anti-HSV-1 IgG, we affinity-purified HSV-1 specific IgG from human intravenous immunoglobulin (starting with a pure clinical IgG preparation), and mixed the purified IgG into CVM samples that had low endogenous anti-HSV-1 IgG. We found that addition of 1 μg/mL anti-HSV-1 IgG trapped HSV-1 with potency comparable to that of endogenous anti-HSV-1 IgG (Fig. 2.3, $p < 0.05$ compared to native specimen without addition of anti-HSV-1 IgG). We

further tested lower anti-HSV-1 IgG doses, and observed potent trapping of virions when ~333 ng/mL anti-HSV-1 IgG was added ($p < 0.05$), and partial trapping at 100 and 33 ng/mL anti-HSV-1 IgG added (both $p < 0.05$). As controls, muco-adhesive PS remained markedly slowed or immobilized and muco-inert PS-PEG freely diffusive in CVM samples treated with the highest anti-HSV-1 IgG doses (data not shown), confirming that the IgG did not cause HSV-1 trapping by altering mucus viscoelasticity or mesh spacing. Affinity-purified anti-HSV-1 IgG exhibited little neutralizing activity at 1 μg/mL and ~333 ng/mL (Fig.2.3 B), based on reduction of plaque formation in Vero cells, suggesting that multiple low-affinity bonds between IgG and CVM can trap virions at IgG levels lower than those needed to neutralize. HSV-1 was also trapped by adding the humanized monoclonal anti-gD IgG in CVM but not by control, non-specific IgG (data not shown), underscoring the specificity of trapping via particular antibody-virus pairs, rather than a non-specific interaction or alteration of general mucus barrier properties.

We next sought to determine the biochemical basis of the low-affinity bonds between IgG and CVM. The Fc domain of all IgGs harbors a conserved N-glycosylation site at Asn297, and many IgG effector functions are Fc- and Asn297 glycan-dependent (Ha et al., 2011). Thus, we prepared $F(ab')_2$ fragments (Fig.2.4 A) and deglycosylated IgG (Fig. 2.4 B) from the same affinity-purified anti-HSV-1 IgG to minimize any changes in HSV-1 binding avidity (confirmed by ELISA), and measured the mobility of HSV-1 pre-mixed with these modified analogs prior to addition to CVM (premixed to minimize interference by endogenous HSV-1 specific IgG). We found both $F(ab')_2$ and deglycosylated IgG exhibited substantially reduced trapping potency compared to intact IgG (Fig. 2.4 C; $p < 0.05$), suggesting that the low-affinity bonds IgG forms with mucins are not only Fc-dependent, but also influenced by Fc glycosylation.

To determine whether trapping viruses in mucus can protect against infection *in vivo*, we evaluated the ability of a non-neutralizing monoclonal IgG to reduce HSV-2 transmission in the pH neutral (Meysick and Garber, 1992) mouse vagina. This monoclonal IgG binds to the relatively sparse gG surface glycoprotein, and exhibited no neutralization activity across all concentrations tested *in vitro* (Fig. 2.5 A). We challenged mice vaginally with 2 ID_{50} HSV-2 with and without anti-gG IgG, and assayed HSV infection by detection of virus shedding in vaginal lavages three days post inoculation, a more sensitive assay of infection than visual observation of lesions, viral isolation from sacral ganglia, or death (Zeitlin et al., 1997). Anti-gG IgG, at a concentration of 3.3 µg/mL and above, significantly protected against infection and reduced the average viral load compared to either medium alone or control, non-specific IgG (Fig. 2.5 A, $p < 0.05$). Furthermore, in mice that received a gentle vaginal lavage to remove mucus without detectable damage to the epithelium (Fig. 2.5 B), anti-gG IgG failed to provide statistically significant protection compared to the corresponding control (Fig. 2.5 C). These findings suggest that, by trapping pathogens in mucus, even a monoclonal, non-neutralizing IgG against a relatively sparse surface antigen can afford substantial protection at mucosal surfaces *in vivo*. Non-neutralizing monoclonals against more prevalent surface antigens, such as gD and gB, or those optimized for trapping pathogens in mucus are likely to provide even more potent protection.

The first evidence of antibody-mucin affinity can be traced back more than 30 years, when Kremer and Jager noted that infertility in humans is often caused by anti-sperm antibodies (Jager et al., 1981; Kremer and Jager, 1976). In cervical mucus samples with high levels of anti-sperm Ab, they found that individual or agglutinated sperm make no forward progress and shake in place for hours until they die, despite vigorous flagellar motility. More recently, Phalipon *et*

al. suggested secretory IgA can aggregate pathogenic *Shigella flexneri* in mouse nasal mucus secretions via the secretory component, anchoring the bacteria to the mucus gel and thereby 'excluding' them from infectious entry (Phalipon et al., 2002). In both instances, the authors assumed that the antibodies were attached firmly to the mucins. Similarly, the mucin-like Fc gamma binding protein (FcyBP) has been proposed to serve an immunological role in mucus through its ability to bind strongly to IgG Fc (Kobayashi et al., 2002). Nevertheless, repeated efforts have failed to detect any significant binding of individual Ab to mucins (Clamp, 1977; Cone, 1999; Crowther et al., 1985; Olmsted et al., 2001; Saltzman et al., 1994). Indeed, FRAP experiments revealed that IgG and other Ab diffuse rapidly in human cervical mucus, slowed only slightly compared to their diffusion in water and with no immobilized (strongly bound) fraction detected (Olmsted et al., 2001). This suggests few if any individual Ab are tightly bound to mucus, and thus viruses cannot be trapped by a single high affinity crosslink between one virion-bound IgG and mucin. By examining the effect of IgG on virions in mucus gel rather than probing directly for interactions between individual IgG molecules and mucins, we were able to document not only the potent trapping of individual virions by multiple surface-bound IgG, but also that the IgG-mucin interactions are Fc- and glycan-dependent

Trapping virions in genital tract mucus should markedly reduce heterosexual transmission of viral infections. Women acquire many of the major sexually transmitted viral infections (e.g., HIV, HPV, and HSV) at rates on the order of 1 per 100 to 1,000 sex acts on average. This suggests few if any of these virions are able to infect target cells per intercourse, and therefore any reduction in the flux of virions that reach target cells should proportionally reduce transmission rates. Blocking initial infection altogether, rather than attempting to clear initial infections, is especially critical for infections that are difficult, if not impossible, to cure

once established. Indeed, our work raises the possibility that the moderate success of RV144 may have been due in part to the vaccine inducing secreted Ab that trapped HIV in CVM and thereby limited the flux of virions that reached target cells. Although the vaccine induced serum HIV-reactive Ab in 99% of participants, *mucosal* levels of the Ab were not monitored, and were likely substantially less, which may explain the moderate 31% vaccine efficacy (26% in men, 39% in women) observed (Rerks-Ngarm et al., 2009); investigations of the mucosal Ab response to the RV144 vaccine are ongoing (Kresge, 2011). Our findings motivate developing vaccines that elicit sufficient secreted Ab to trap pathogens in mucus in addition to eliciting neutralizing titers of systemic Ab. Secreted Ab that bind to 'non-neutralizing' surface epitopes should trap pathogens as effectively as those that bind to neutralizing epitopes, a prospect that may broaden potential antigen targets for vaccine development, especially against virions with rapidly evolving neutralizing epitopes.

Fc-mediated trapping of pathogens in mucus, which directly blocks infections at the portals of entry, may represent an exceptionally potent mechanism by which the immune system can rapidly adapt and reinforce multiple mucosal surfaces against diverse and rapidly evolving pathogens. In pilot studies, we found LPS-specific monoclonal IgG immobilized individual *Salmonella typhimurium* in mucus secretions lining mouse gastrointestinal tract tissues without inhibiting the flagella beating apparatus and without causing aggregation (i.e., independent of the classical, aggregation-based mechanism of immune exclusion; unpublished data, Subramani, Lai). In contrast, *Salmonella* rapidly penetrated control mucus gel. The observed trapping in both CVM (predominantly Muc5b mucins) and gastrointestinal mucus (Muc2 mucins) suggests the molecular basis for Fc-mucin affinity is likely common among major secreted mucins – the long densely glycosylated fibers that form mucus gels – and

possibly mediated by glycans, since sugars represent the major constituent of mucins (up to 80% by dry weight (Lai et al., 2009b)). Nevertheless, significant technical challenges remain in elucidating the precise entities on mucins responsible for the observed Fc-mucin affinity because biochemical perturbations of the mucus gel typically destroy the native mucin mesh microstructure and gel viscoelasticity (Kocevar-Nared et al., 1997) needed to trap pathogens in the gel. Improved understanding of the molecular basis of Fc-mucin affinity will likely offer critical insight into understanding and identifying subpopulations with greater susceptibility to infection, as well as therapeutic strategies to enhance this mucosal immune protective mechanism.

2.3 MATERIALS AND METHODS

2.3.1 Culture and purification of fluorescent HSV-1

The HSV-1 mutant 166v (Elliott and O'Hare, 1999), encoding a VP22-Green Fluorescent Protein (GFP) tegument protein packaged into HSV-1 at relatively high copy numbers (Heine et al., 1974), was kindly provided by Richard Courtney and utilized in all microscopy and ELISA studies, besides those for *in vivo* experiments. The addition of GFP to the VP22 protein appears to have no deleterious effects on viral replication (Elliott and O'Hare, 1999), and the fluorescence of 166v was consistently more intense than that of HSV-1 mutants encoding other GFP fusion proteins. 166v was expanded at an MOI of 3 on confluent monolayers of HaCat cells maintained in DMEM (Life Technologies, Grand Island, NY) supplemented with 5% FBS, 1x L-glutamine and 1x Penicillin/Streptomycin. Culture medium was collected 16-18 hr post-infection and twice centrifuged at 1000 xg for 5 min to remove cell debris. The resulting supernatant was split into 30 mL aliquots and precipitated overnight with a polyethylene glycol (PEG)/salt solution. Briefly, 10 mL of 1.55 M NaCl was added to 30 mL of crude virus supernatant, followed by 10

mL of 40% PEG 8000 (Sigma, St. Louis, MO). After an overnight incubation at 4°C the virus/PEG solution was centrifuged at 2555 xg and 4°C for 1 hr. The virus pellet was then resuspended in 1x PBS and centrifuged through a continuous 20-50% (w/w) sucrose in PBS gradient for 1 hr at 74,119 xg. The resulting virus band was collected, diluted 1:5 in PBS, layered over 30% (w/w) sucrose in PBS, and centrifuged for 1.5 hr at 83,472 xg to pellet virus for further purification. Purified virus pellet was resuspended in PBS and stored as single use aliquots at –80°C.

2.2.2 Cervicovaginal mucus (CVM) collection and characterization

CVM collection was performed as published previously (Lai et al., 2009a; Lai et al., 2010). Briefly, undiluted CVM secretions, averaging 0.3 g per sample, were obtained from women of reproductive age, ranging from 20 to 32 years old (27.4 ± 0.9 years, mean ± SEM), by using a self-sampling menstrual collection device following protocols approved by the Institutional Review Board of the University of North Carolina – Chapel Hill. Informed consent of participants was obtained after the nature and possible consequences of the study were explained. The device was inserted into the vagina for at least 30 s, removed, and placed into a 50 mL centrifuge tube. Samples were centrifuged at 230 xg for 2 min to collect the secretions. Aliquots of CVM for lactic acid and Ab measurements (diluted 1:5 with 1x PBS and stored at –80°C) and slides for gram staining were prepared immediately, and the remainder of the sample was stored at 4°C until microscopy, typically within a few hours. Samples were collected at random times throughout the menstrual cycle, and cycle phase was estimated based on the last menstrual period date normalized to a 28 day cycle. No samples were ovulatory based on visual observation (none exhibited spinnbarkeit). Samples that were non-uniform in color or consistency were discarded. Donors stated they had not used vaginal products nor participated in

unprotected intercourse within 3 days prior to donating. All samples had pH <4.5; none had bacterial vaginosis (BV) based on Gram staining and Nugent scoring, following scoring criteria described previously (Nugent et al., 1991). For lactic acid and Ab measurements, CVM aliquots were thawed and centrifuged for 2 min at 21,130 xg to obtain cell-free supernatant containing lactic acid and Ab. Lactic acid content was measured using a D-/L-lactic acid kit (R-Biopharm, Darmstadt, Germany) according to manufacturer protocol, but adapted to a 96-well format.

Total immunoglobulin levels in CVM were quantified using the Human Isotyping Kit (HGAMMAG-301K; Millipore, Billerica, MA) according to manufacturer protocol. Briefly, 20X stock isotyping beads were vortexed, sonicated, diluted to 1X, and incubated with 50 µL of serially diluted CVM supernatant at 1:2 beads:CVM volume ratio. After 1hr, the beads were separated from CVM supernatant using a magnetic plate, and washed twice with wash buffer. The beads were then incubated with 25 µL of 1X anti-Human Kappa and Lambda-PE for 1 hr, washed twice, and resuspended in Luminex Drive fluid. Fluorescence intensities indicative of immunoglobulin levels present in CVM were measured using the Luminex MAGPIX system, and data analysis was performed using Milliplex Analyst (v3.5.5.0; Vigene Tech Inc., Carlisle, MA). All incubations were carried out at room temperature in the dark with vigorous agitation.

Whole-virus ELISA was used to quantify HSV-1 specific IgG. Briefly, high-affinity 96-well half-area plates (Thermo Scientific, Rockford, IL) were coated overnight at 4°C with 25 µL per well of affinity-purified intact HSV-1 at 20 µg/mL (measured using BCA assay). The plates were washed four times with 0.05% Tween in PBS (PBS-T), blocked with 5% milk for at least 1 hr followed by PBS-T washes, then incubated for at least 1 hr with serial dilutions of CVM supernatant. Following PBS-T washes, virion-bound IgG was quantified using $F(ab')_2$ anti-human IgG Fc (Goat)-HRP conjugate (709-1317; Rockland, Gilbertsville, PA) and 1-Step Ultra

TMB substrate (Thermo Scientific, Rockford, IL), and compared to a standard generated on the same plate using twice-purified anti-HSV-1 IgG, which we assumed to be >90% pure. TMB conversion was terminated with 2 N sulfuric acid, and absorbance was measured at 450 nm using a BioTek Synergy 2 plate reader. HSV-1 specific IgA and IgM levels were too low to be detected by our assay.

2.2.4 Preparation and characterization of anti-HSV-1 IgG

Anti-HSV-1 IgG was purified from intravenous immunoglobulin (IVIg, Privigen®; ≥ 98% IgG; CSL Behring, King of Prussia, PA) by affinity column purification. Briefly, HSV glycoproteins were extracted from purified HSV-1 by overnight incubation with Triton X-100 (final concentration 0.05%) at 4°C, followed by centrifugation at 21,130 xg and 4°C for 1.5 hr. The resulting supernatant containing HSV glycoproteins was coupled to AminoLink Plus Coupling Resins (Thermo Scientific, Rockford, IL) according to manufacturer protocol, and stored at 4 °C until use. To extract HSV-1 specific IgG, the column was first warmed to room temperature and washed twice with 3 mL of equilibrium buffer (150 mM NaCl, 0.05% Tween, 10 mM sodium phosphate at pH 6). The column was then loaded with 2 mL of IVIg buffer exchanged into equilibrium buffer using a 50 kDa MWCO concentrator (Corning, Tewksbury, MA), and incubated at room temperature for at least 45 min with end-over-end mixing. Unbound, non-specific Ab was removed by washing with 1 mL of equilibrium buffer followed by three additional rounds of wash buffer (4 mL each round; 500 mM NaCl, 0.05% Tween, 10 mM sodium phosphate at pH 6). Bound Ab was then eluted using IgG Elution Buffer (Thermo Scientific, Rockford, IL); each elution consisted of three 3 mL volumes of elution buffer, and was collected into tubes containing 100 µL of 10 mM sodium phosphate pH 6 to neutralize the elutions. Elutions from multiple runs were pooled together, concentrated and buffer exchanged

into PBS using a 30 kDa MWCO concentrator tube, supplemented with sodium azide (final concentration 0.03%) and stored at 4°C until use. A single purification round removed over 99% of non-specific IgG, tested by spiking IVIg with mouse IgG. Final concentration of purified IgG was measured via sandwich ELISA, with plates coated with 2 µg/mL of anti-human IgG Fc (Alpha Diagnostics, San Antonio, TX) followed by detection with $F(ab')_2$ anti-human IgG Fc (Goat)-HRP, and compared to a standard curve generated with serial dilutions of stock IVIg.

2.2.4 Preparation and characterization of anti-HSV-1 F(ab')2

HSV-1 specific IgG was fragmented using a $F(ab')_2$ Preparation Kit (Thermo Scientific, Rockford, IL). Briefly, IgG was desalted into IgG Digestion Buffer using 3 kDa MWCO concentrator tubes (Amicon 0.5 mL; Millipore, Billerica, MA) and incubated with pepsin at 37°C for 3.5 hr with end-over-end mixing, followed by purification using a Protein A column (0.2 mL resin; Thermo Scientific, Rockford, IL) and PBS washes to remove undigested IgG. Fragmentation was confirmed using a non-reducing 4-12% Bis-Tris gel with MOPS running buffer. The gel was stained with Coomassie Blue for imaging; note that the gel image presented in Fig. 4 and Fig. S3 was desaturated and contrast-adjusted using Pixlr photo editor to produce a black and white image (same settings applied across entire image). A competitive inhibition ELISA was also performed to confirm that the purified $F(ab')_2$ blocked binding of intact anti-HSV-1 IgG. HSV-1 coated wells were incubated with either 1% milk or different dilutions of anti-HSV-1 $F(ab')_2$ for 1 hr, followed by incubation with intact HSV-1 specific IgG for 1 hr and quantification of bound IgG using $F(ab')_2$ anti-human IgG Fc (Goat)-HRP conjugate. Total amounts of anti-HSV-1 $F(ab')_2$ were quantified via sandwich ELISA with plates coated with HSV-1 virions as described above, but with detection by anti-human IgG $F(ab')_2$ (Goat)-HRP conjugate (Rockland 209-1304).

2.2.5 Preparation and characterization of deglycosylated anti-HSV-1 IgG

N-linked oligosaccharides on purified anti-HSV-1 IgG were cleaved by incubating 200 µg of IgG with 10 µL of PNGase and 11 µL of 10x G7 reaction buffer (New England Biolabs, Ipswich, MA) for at least 24 hr at 37°C. IgG was then recovered using a Protein A column, eluted with IgG Elution Buffer into 100 µL of 10 mM sodium phosphate pH 6 and buffer exchanged into PBS using a 30 kDa MWCO concentrator tube. The deglycosylated IgG was further purified using a 0.8 mL spin column immobilized with Con A-agarose slurry (Vector Labs, Burlingame, CA) and washed thrice with equilibrium buffer (10 mM HEPES with 0.15 M NaCl at pH 7.5) prior to incubation with end-over-end mixing for 45 min at room temperature. Following the incubation, the column was spun at 5000 xg for 1 min to collect the flow through, which contains the deglycosylated IgG, and washed thrice with equilibrium buffer to maximize recovery. The flow through and the washes were pooled, buffer exchanged into PBS using a 30 kDa MWCO concentrator tube, supplemented with sodium azide (final concentration 0.03%) and stored at 4°C until use. Total amounts of deglycosylated IgG were measured as described above. Deglycosylation was confirmed using a lectin-ELISA assay. Briefly, high-affinity 96-well plates were coated overnight at 4°C with 50 µL per well of 1 µg/mL purified deglycosylated HSV-1 IgG. The plates were washed 4x with PBS-T, blocked with 300 µL/well of 1x Carbo Free solution (Vector Labs, Burlingam,CA) for at least 1 hr followed by PBS-T washes, then incubated with 50 µL/well of 1 µg/mL biotinylated Con A lectin (Vector Labs, Burlingam, CA) for at least 2 hr. Following PBS-T washes, IgG-bound lectin was quantified using anti-biotin-HRP conjugate (Vector Labs, Burlingame, CA) and 1-Step Ultra TMB substrate, and compared to wells coated with affinity-purified HSV-1 IgG or IVIg. TMB conversion was terminated with 2 N sulfuric acid, and absorbance was measured at 460 nm using a BioTek Synergy 2plate reader

and normalized to the amount of IgG bound to coated wells quantified using $F(ab')_2$ anti-human IgG Fc (Goat)-HRP conjugate.

2.2.6 Neutralization assay

Purified HSV-1 (~550 PFU; 5 µL) was incubated with 95 µL of HSV-1 specific IgG solution at different final concentrations for 1 hr with end-over-end mixing. The mixture was then diluted with 210 µL of media, of which duplicate 150 µL aliquots were transferred to confluent Vero cell monolayers in a 6-well plate. Plates were incubated at 37 °C for 1 hr with periodic rocking to ensure that the plates did not dry out, before the HSV-1/Ab mixture was aspirated off and wells were washed with 2 mL of PBS. The plates were then incubated for 3 days at 37°C in 2% carboxymethyl cellulose in EMEM supplemented with 1x L-glutamine and 1x Penicillin/Streptomycin, before staining with 1% crystal violet solution, and the resulting plaques were manually counted and compared to control wells to determine the extent of neutralization.

2.2.7 Multiple particle tracking of HSV-1 in CVM

To mimic neutralization of CVM by alkaline seminal fluid, we titrated CVM to pH 6.8-7.1 using small volumes (~3% v/v) of 3 N NaOH, and confirmed pH using a micro pH electrode (Microelectrodes, Inc., Bedford, NH) calibrated to pH 4, 7 and 10 buffers. Samples were either untreated or treated by addition of known amounts of purified anti-HSV-1 IgG or control (anti-biotin) IgG. Control beads consisted of red or green fluorescent 200 nm carboxyl-modified polystyrene particles (Molecular Probes, Eugene, OR), either uncoated (PS; muco-adhesive) or covalently conjugated with low molecular weight (2 kDa), amine-functionalized polyethylene glycol (PEG; Rapp Polymere, Tuebingen, Germany) to produce coated particles (PS-PEG; muco-inert), as previously described (Lai et al., 2007). Fluorescent virions or control beads

(approximately 10^8–10^9 particles/mL) were added at 5% v/v to 20 μL of CVM placed in a custom-made glass chamber, and incubated for 1 hr at 37°C prior to microscopy. The translational motions of the particles were recorded using an EMCCD camera (Evolve 512; Photometrics, Tucson, AZ) mounted on an inverted epifluorescence microscope (AxioObserver D1; Zeiss, Thornwood, NY), equipped with an Alpha Plan-Apo 100x/1.46 NA objective, environmental (temperature and CO_2) control chamber and an LED light source (Lumencor Light Engine DAPI/GFP/543/623/690). Videos (512 x 512, 16-bit image depth) were captured with MetaMorph imaging software (Molecular Devices, Sunnyvale, CA) at a temporal resolution of 66.7 ms and spatial resolution of 10 nm (nominal pixel resolution 0.156 μm/pixel) for 20 s. Particle trajectories were analyzed using MetaMorph software as described previously (Lai et al., 2009a; Lai et al., 2007; Lai et al., 2010); image contrast was adjusted to improve particle visibility, but the same contrast level was applied throughout the entire video and did not bias toward any particle population. Trapped particles were defined as those with effective diffusivity (D_{eff}) < 0.01 $\mu m^2/s$ at a time scale (τ) of 1 s (i.e., particles move less than their diameter within 1 s). In a subset of experiments, we confirmed that particles defined as trapped over the course of 20 s based on this criterion remain confined to the same locations over more than 15 min. At least five independent experiments in CVM from different donors, with n ≥100 particles per experiment, were performed for each condition. For a subset of donors, similar observations were made at least twice in samples obtained on separate days to ensure reproducibility, but only one sample was used for analysis.

2.2.8 Mouse vaginal HSV-2 challenge model

All experiments conducted with mice were performed in accordance with protocols approved by the Johns Hopkins University Animal Care and Use Committee satisfying the

requirements of the E.E.C. Guidelines (1986) and U.S. Federal Guidelines (1985). Female CF-1 mice (6-8 weeks old; Harlan, Frederick, MD) were treated with Depo-Provera® (medroxyprogesterone acetate, 2.5 mg/mouse) by subcutaneous injection into the right flank 6-8 days prior to use. Depo-Provera® synchronizes mice in a prolonged diestrus-like state, in which the vaginal epithelium thins and susceptibility of the tissue to infection increases (Cone et al., 2006). Depo-Provera®-treated mice were randomly divided into groups of ten. The mouse vagina is pH neutral (Meysick and Garber, 1992); therefore, we did not attempt to modify vaginal pH prior to inoculation. Inocula were prepared by mixing HSV-2 (final dose 2 ID_{50}; strain G, ATCC, Manassas, VA) with medium or different concentrations of control (anti-biotin) or anti-gG IgG (8.F.141; Santa Cruz Biotechnology, Inc., Santa Cruz, CA), and incubating for 1 hr at 37°C. Mice were inoculated with 20 µL of HSV-2 solution, delivered to the vagina using a 50 µL Wiretrol (Drummond, Broomall, PA), fire-polished to avoid damage to the vaginal epithelium. In some studies, the mouse vagina was gently washed with ~10 mL of normal saline delivered at 1 mL/min through a smooth ball-tipped gavage needle connected to a syringe pump, prior to HSV-2 challenge. Removal of mucus by this process was measured using a fluorimetric mucin assay, as previously described (Crowther and Wetmore, 1987). Importantly, the gentle wash did not damage the vaginal epithelium, as confirmed by microscopy with a fluorescence-based dead cell stain (YOYO-1) that assesses membrane integrity (Cone et al., 2006), compared to conventional lavage and/or vaginal swabbing with a cotton tip, which induced significant epithelial damage. YOYO-1 has been previously used to reveal toxicity caused by detergent-based microbicides that led to increased susceptibility to HSV infection (Cone et al., 2006). Infection was assayed three days post-inoculation by detection of virus in vaginal lavages. Briefly, 50 µL of medium was pipetted in and out of the vagina 20 times, diluted to 0.2 mL and

placed on target cells (ELVIS® HSV Test System; Diagnostic Hybrids, Athens, OH); infected cells (foci) were identified one day later, following manufacturer protocol. Scores for virus shedding were assigned on a scale of 0-4 based on the approximate density of foci observed ("0": 0; "0.5": <100; "1": 100-500; "2": 500-1000; "3": 1000+; "4": saturated). At least three independent experiments were performed for each condition, with n = 10 animals per experimental group ($n \geq 30$ total).

2.2.9 Statistical analysis

Correlation between endogenous anti-HSV-1 IgG levels and average particle or virus D_{eff} in individual CVM samples was measured using Pearson's correlation coefficient (r). Statistical comparisons were limited to two groups (test group compared with the appropriate control group performed during the same experiment). Fisher's exact test was used to determine the statistical significance of reductions in % mice infected. A two-tailed Student's t-test (paired for comparisons of Ab-treated vs. native CVM for the same CVM samples) was used for all other comparisons. Differences were deemed significant at an alpha level of 0.05. All values are reported as mean ± SEM unless otherwise indicated.

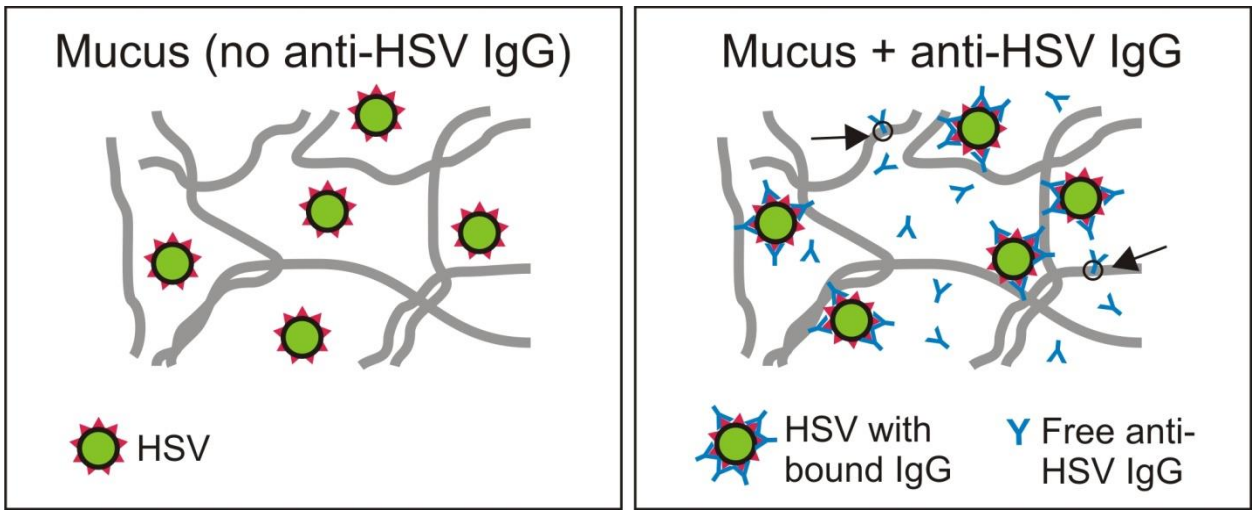

Figure 2.1 Proposed mechanism of Ab-mediated trapping of viruses in mucus. Schematic showing (A) HSV readily penetrates native CVM with little to no endogenous anti-HSV IgG, and (B) anti-HSV IgG traps HSV in CVM by multiple transient, low affinity bonds with mucins. By forming only short-lived, low-affinity bonds with mucus, free Ab, such as IgG, are able to diffuse rapidly through mucus and bind to viruses. As IgG molecules accumulate on the virus surface, they form multiple low-affinity bonds between the virus and mucus gel. A sufficient number of these transient low-affinity bonds ensure viruses are effectively trapped in mucus at any given time, thereby reducing the flux of infectious virions that can reach target cells. In a similar fashion, IgM, with its 10 relatively low-affinity Fab components, is well known to make essentially permanent polyvalent 'high avidity' bonds. Arrows indicate the small fraction of free (not virus-bound) IgG (~10-20%) that will interact with mucins at any moment in time (Cone, 1999; Olmsted et al., 2001).

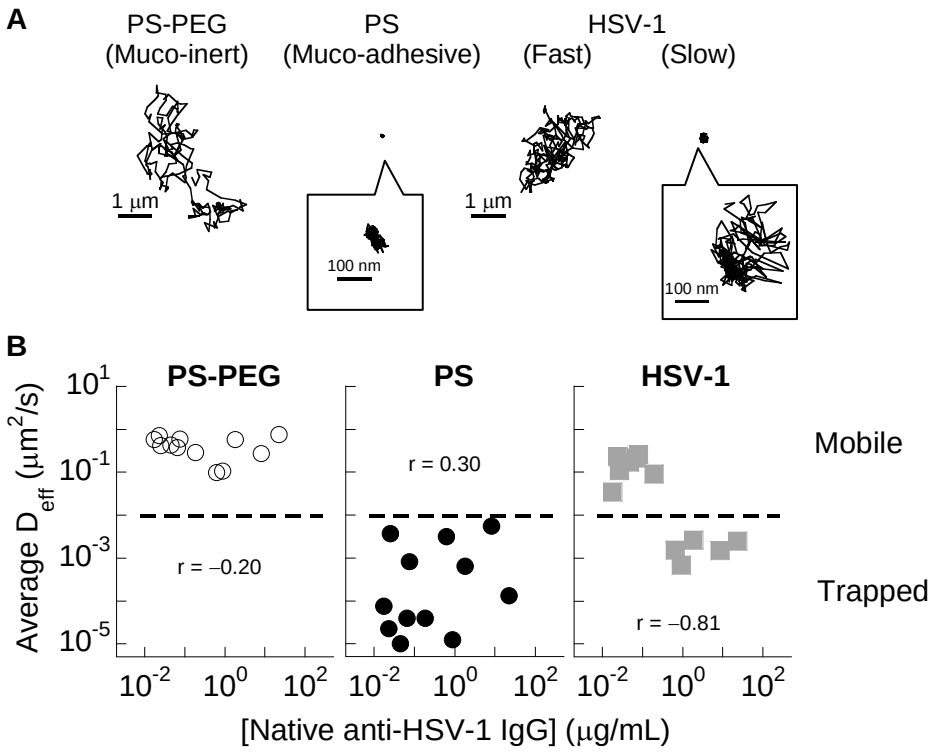

Figure 2.2 HSV-1 is immobilized in CVM samples with elevated endogenous anti-HSV-1 IgG but readily mobile in samples with low endogenous anti-HSV-1 IgG. Fluorescent HSV-1 or control particles were added to CVM, and their motions were analyzed by multiple particle tracking methods. (A) Representative 20 s traces of HSV-1 (d ~180 nm) and control particles (d ~200 nm) with effective diffusivity (D_{eff}) at a time scale τ of 1 s within one SEM of the mean. Control particles include muco-inert (PEG-coated; PS-PEG) and muco-adhesive (uncoated; PS) polystyrene beads, which are freely diffusive and trapped in human CVM, respectively, as previously shown (Lai et al., 2007). (B) Geometric average D_{eff} (τ = 1 s) for PS-PEG, PS and HSV-1 in individual CVM samples from unique donors (n = 12, each experiment performed independently) as a function of endogenous anti-HSV-1 IgG. Dashed lines represent the D_{eff} cutoff below which particles are permanently trapped (moving less than their diameter within 1 s). Pearson's correlation coefficients (r) are indicated.

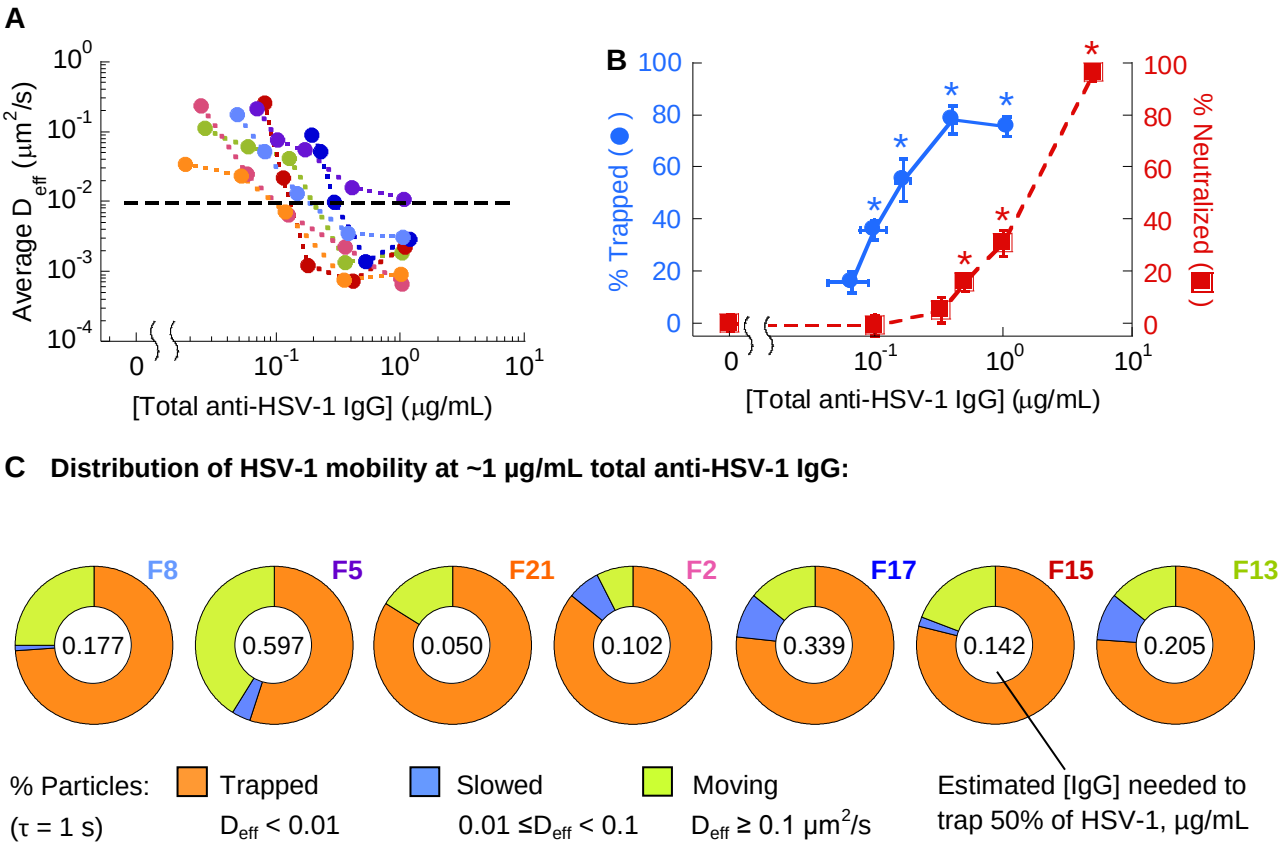

Figure 2.3 Anti-HSV-1 polyclonal human IgG added to CVM samples with low endogenous anti-HSV-1 IgG potently traps HSV-1. HSV-1 mobility was quantified in aliquots of the same CVM samples with different amounts of anti-HSV-1 IgG added. (A) Comparison of effective diffusivity (D_{eff}; τ = 1 s) for HSV-1 in CVM samples (n = 7, each experiment performed independently) with different amounts of total anti-HSV-1 IgG (sum of endogenous and added IgG). Different colored circles represent distinct samples. (B) *In vitro* neutralization vs. trapping potency of anti-HSV-1 IgG. Neutralization was assayed based on reduction of HSV plaque formation in Vero cells; trapping was defined as D_{eff} (τ = 1 s) below 0.01 $\mu m^2/s$. See Materials and Methods for additional details. Total IgG was averaged across samples for each treatment group. Error bars represent SEM. * indicates statistically significant difference compared to respective controls ($p < 0.05$). (C) Distribution of particle speeds in samples treated with 1 μg/mL IgG (annulus chart), and estimated concentration of total IgG (μg/mL) needed for 50% trapping (number in center). Donor ID is indicated for each sample, with colors matching those in (A).

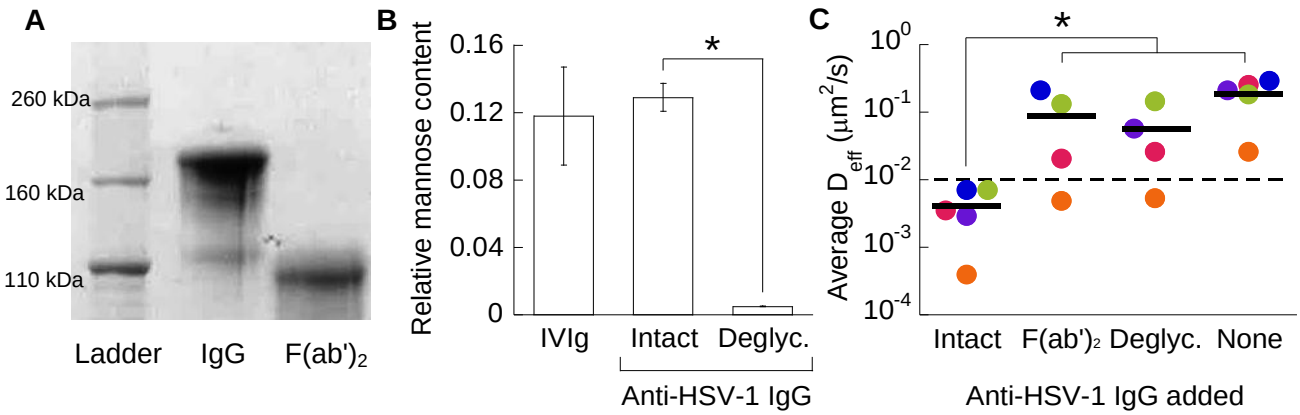

Figure 2.4. IgG-mucin affinity is Fc- and glycosylation-dependent. (A) Preparation of anti-HSV-1 $F(ab')_2$ confirmed by SDS-PAGE; full-length gel is presented in Fig. S3. (B) Preparation of deglycosylated anti-HSV-1 IgG confirmed by lectin-binding assay (absorbance of IgG-bound ConA normalized to amount of IgG). Error bars represent SEM. (C) Mobility (D_{eff}; τ = 1 s) of HSV-1 in CVM with low endogenous anti-HSV-1 IgG incubated with various HSV-1 specific Ab: 1 μg/mL affinity-purified native IgG ("Intact"), 667 ng/mL $F(ab')_2$, and 1 □g/mL deglycosylated IgG compared to HSV-1 in native CVM ("None"). Distinct samples (n = 4-5, each experiment performed independently) are indicated with different color circles; averages are indicated by solid lines. Dashed line represents the D_{eff} cutoff below which particles are permanently trapped (moving less than their diameter within 1 s). * indicates statistically significant difference ($p < 0.05$).

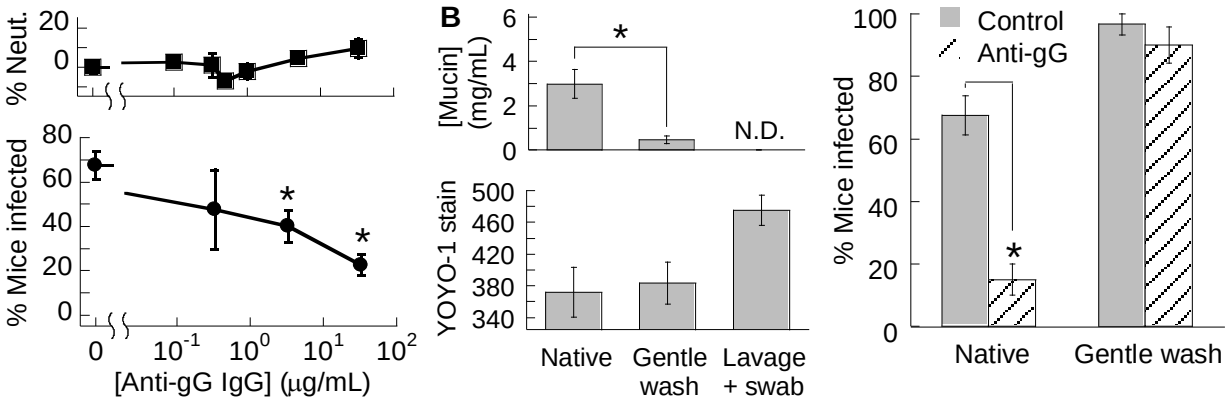

Figure 2.5: A non- neutralizing monoclonal IgG against the gG epitope protects against vaginal HSV-2 infection in mice via IgG-mucus interactions. (A) In vivo protection vs. in vitro neutralization (% Neut.) of HSV-2. Neutralization was assayed based on reduction of HSV plaque formation in Vero cells. Depo-Provera®-treated mice were inoculated with HSV-2 mixed with control or anti-gG IgG. Infection was assayed three days post-inoculation by detection of virus in vaginal lavages using the ELVIS® HSV Test System. (B) Mucin concentration in vaginal fluid collected from the native or gently washed mouse vagina, and YOYO-1 staining for vaginal epithelial cell damage in gently washed or conventionally lavaged and swabbed (cotton tip) mice. N.D. = no data. (C) *In vivo* protection by 33 μg/mL anti-gG IgG is lost when mouse CVM is removed by gentle washing using a syringe pump. Data represent at least three independent experiments, each with n = 10 mice per group (*in vivo*; total n = 40 per group for data in (A), n ≥ 30 for (C)) or performed in triplicate (*in vitro*). Error bars represent SEM. * indicates statistically significant difference compared to control ($p < 0.05$).

Donor ID	Cycle day[1]	Cycle phase[3]	Nugent score[4]	% Lactic acid[5]
F10	17	Luteal	1	2.4 ± 0.039
F12	25	Luteal	2	0.81 ± 0.081
F14	26	Luteal	2	0.95 ± 0.10
F18	11	Follicular	4	0.56 ± 0.022
F9	N/A[2]	N/A	0	0.93 ± 0.062
F13	9	Follicular	0	1.1 ± 0.031
F15	25	Luteal	0	1.1 ± 0.042
F17	N/A	N/A	1	1.2 ± 0.088
F2	15	Luteal	2	0.74 ± 0.073
F21	N/A	N/A	0	1.5 ± 0.081
F5	10	Follicular	0	1.4 ± 0.074
F8	19	Luteal	0	1.9 ± 0.15
		Median	**0.5**	**1.10**
		SEM	**0.37**	**0.15**

Table 2.1: Characterization of CVM samples: menstrual cycle phase, nugent score and % lactic acid

[1]Cycle day calculated as the number of days from the first day of the last menstrual period normalized by the cycle length to a 28 day cycle. [2]N/A = hormonal contraceptive. [3]Cycle phase estimated based on normalized cycle day; no samples were ovulatory based on absence of spinnbarkeit by visual inspection. [4]A Nugent score of 0-3 corresponds to "normal" (lactobacilli-dominated) microflora, 4-6 to "intermediate", and 7-10 to "bacterial vaginosis" (BV) – a condition associated with greater risk of STI acquisition. Assessment of Nugent scores was independently confirmed by the Clinical Microbiology and Immunology Lab at UNC. [5]Values are expressed as mean ± SEM. Grey highlight indicates CVM samples containing sufficient native levels of anti-HSV-1 IgG to immobilize virions.

Donor ID	Anti-HSV-1 IgG		IgG_1	IgG_2	IgG_3	IgG_4	Total IgG	Total IgA	Total IgM
	Average	% of							
F10	0.92 ± 0.20	0.60%	90%	6.7%	3.4%	N.D.[2]	150 ± 12	1.0 ±	2.1 ± 1.7
F12	0.66 ± 0.037	0.19%	65%	28%	8.1%	0.66%	360 ± 36	8.1 ±	1.2 ± 0.91
F14	1.9 ± 0.20	0.14%	78%	19%	4.2%	1.0%	1300 ±	79 ± 9.3	4.8 ± 0.11
F18	8.5 ± 0.31	0.56%	71%	20%	6.1%	4.5%	1500 ±	200 ±	72 ± 6.9
F9	23 ± 1.4	1.2%	83%	11%	4.0%	1.5%	1900 ±	150 ±	39 ± 5.5
Median	**1.9**	**0.56%**	**78%**	**19%**	**4.2%**	**1.0%**	**1300**	**79**	**4.8**
SEM	**4.3**	**0.19%**	**4.3%**	**3.7%**	**0.88%**	**0.77%**	**340**	**38**	**14**
F13	0.026 ±	0.027%	76%	18%	5.7%	0.28%	980 ± 79	7.0 ±	2.9 ± 1.3
F15	0.080 ±	0.024%	68%	29%	4.1%	0.28%	330 ± 43	5.0 ±	1.4 ± 0.92
F17	0.19 ± 0.023	0.036%	49%	34%	20%	0.67%	540 ± 33	17 ± 1.5	3.3 ± 0.59
F2	0.025	0.0044%	67%	27%	9.2%	0.0044%	560 ± 40	8.9 ±	3.8 ± 0.44
F21	0.018 ±	0.013%	70%	27%	4.0%	0.056%	140 ±	4.0 ±	0.085 ±
F5	0.070 ±	0.010%	91%	6.4%	1.9%	0.41%	680 ± 49	3.0 ±	1.7 ± 1.2
F8	0.048 ±	0.036%	67%	28%	5.0%	0.021%	130 ±	2.1 ±	1.4 ± 1.2
Median	**0.048**	**0.013%**	**68%**	**27%**	**5.0%**	**0.28%**	**540**	**5.0**	**1.7**
SEM	**0.023**	**0.0053%**	**4.7%**	**3.4%**	**2.3%**	**0.092%**	**110**	**1.9**	**0.49**

Table 2.2: Characterization of CVM samples: Ab content

[1]Values are expressed as mean ± SEM; all Ab concentrations are expressed in units of μg/mL except for those of different subclasses of IgG, which are expressed as % of total IgG. Data represent at least two independent measurements, in duplicate. Values that fell outside the range of the assay were not included, which in some cases led to totals across IgG subclasses of greater than 100% after averaging across measurements. [2]N.D. = not detected (below threshold). Grey highlight indicates CVM samples containing sufficient native levels of anti-HSV-1 IgG to immobilize virions.

CHAPTER 3

ROLE OF IgG-FC N-GLYCOSYLATION IN IgG-MUCIN CROSSLINKING

3.1 INTRODUCTION

Nearly all IgG have complex N-linked glycans present at the Asn297 site of its Fc domain (Figure 3.1A); N-glycans often influence many of the IgG effector functions. As we have shown in the previous chapter, IgG mediated trapping of individual HSV virions appeared to be Fc- and N-glycan- dependent. In this chapter, we sought to further determine and analyze the exact role of this N-glycosylation profile on IgG's ability to immobilize individual viruses in mucus. Elucidating the precise role of N-glycans in IgG-mucin interactions can help us begin to understand whether this mechanism of mucosal immunity may be compromised by specific diseases and/or microbes, as well as engineer more potent prophylactic IgG as microbicides against different sexually transmitted infections.

The primary glycan structure present in Fc-IgG is a heptasaccharide biantennary structure. It contains a common core structure (shown in the boxed region in figure 2.1B), which consists of two N-acetyl glucosamine (GlcNAc) linked serially to asparagine 297 through an amide bond. The other end of the GlcNAc is connected to a mannose residue which branches off into two arms where each arm contains a mannose and GlcNAc. The sugars present outside of the boxed region, galactose, sialic acid, fucose and bisecting GlcNAc, represent the terminal sugars that contribute to much of the variations in IgG-Fc glycosylation. The presence or absence

of these sugars lead to the structural heterogeneity of Fc glycans, and consequently Fc-effector functions. Figure 1C shows the different N-glycoforms present in human IgG Fc (Raju, 2008).

A majority of IVIG is core fucosylated, and the full glycan structure (i.e. G2S2 in Fig. 2.1 C) is only found in ~5% of the IVIG pool. (Kaneko, 2006) The major glycoform present is a

Glycan structure with the core structure and one galactose (G1, with 1,6 fucose) which represents ~39% of the total IVIG pool. (Raju, 2008 and Anumula, 2008) The next predominant glycoform present in the Fc region is the common core structure (also known as the G0 pattern, Fig. 3.1C), which is ~26%. This is followed by a structure where both galactose are present (known as G2, with 1, 6 fucose in Fig. 3.1 C), which is about 20% of the total. (Anumula, 2008 and Raju, 2008). The distribution of these glycoforms varies depending on person's age, gender and overall physical health. For example, serum IgG in young adults have increased galactosylation while with increasing age the galactosylation decreases. In contrast, people with autonimmune diseases, such as rheumatoid arthritis, possess IgG with reduced galactose (and consequently a decrease in siaylation) relative to the common core structure. (Huhn et al., 2009)

In order to determine how the terminal sugars of IgG-Fc affect IgG-mucin affinity, we sought to isolate Herpes-specific IgG with precise glycan patterns. Unfortunately, there are many technical challenges associated with purifying a specific IgG glycoform from a heterogeneous IgG mixture purified from serum includes the poor binding of many lectins to F-glycans, and cross-reactivity between lectins and O-glycans in the Fab region (Anumula, 2012 and Dalziel, 1999). In addition, although many enzymes are available to either add or remove sugar residues from specific glycan structures, these enzymes typically have poor access to the Fc glycans, generally shielded within the Fc core, and therefore have exceedingly poor reaction yield without

denaturing the IgGs. (Kaneko, 2006 and Wang et al., 2011) To circumvent these challenges, we turned to the use of monoclonal antibodies expressed in plants, which is often termed as "plantibodies". These plantibodies can be expressed in plant systems engineered with over-expression or knockout of enzymes/glycotransferrases, and therefore capable of producing large quantities of IgG of a specific human glycosylation patterns. In this chapter, again using HSV-1 in human cervicovaginal mucus (CVM), we explored how the galactose terminated and GlcNAc terminated (shown as AGn/AA and GnGn in Table 3.1, note that these aren't called G1/G2 or G0 due to lack of fucose in plantibodies) exhibits distinct affinity to mucins and consequently different potency in trapping individual HSV virions.

3.2 RESULTS

HSV8, a monoclonal antibody that binds to the gD surface glycoprotein, where the (Fab)'2 was "isolated by antigen selection from a phage-displayed combinatorial antibody library established from a herpes simplex virus (HSV)-seropositive individual". (De Logu et al., 1998) We genetically introduced and expressed the plasmid encoding HSV8 IgG in tobacco plants to generate HSV8 plantibodies with three different glycosylation patterns: GnGn, Galactose (Gal) and Aglycosylated (Agly). The glycosylation patterns were confirmed with MALD-TOF-MS analysis (Table 3.1) as well as lectin blots (data not shown). HSV8-GnGn plantibodies have the core structure as its major glycoform (~90%, see GnGn in Table 3.1), whereas galactosylated plantibodies (HSV8 - Gal) have a major glycoform of core structure plus two galactose (~68%, see AGn and AA in Table 3.1). HSV8-Agly plantibodies had no detectable glycans present (Table 3.1). Human HSV8 expressed and produced in human 293 HEK cells and was included as a positive control.

I added different plantibodies and HSV-1 to pH neutralized CVM, followed by time-lapse microscopy of virion motion in real-time with high spatiotemporal resolution (15 fps; 10 nm tracking resolution). Virion mobility was then quantified using multiple particle tracking. In all three samples, for both control and Plant Agly conditions, HSV-1 exhibited relatively unhindered diffusion in CVM (Figure 3.2). In contrast, in samples treated with Plant GnGn and Human HSV8, most HSV-1 virions were effectively trapped, moving less than their diameter (<200 nm) in 20s (D_{eff} < 0.01 um^2/s). Interestingly, in CVM treated with HSV8-Gal, the diffusion of HSV in two out of the three samples was only somewhat slowed whereas the same CVM specimen treated with HSV8 GnGn possessed greater trapping potency. Human HSV8 and HSV8-GnGn treated CVM samples significantly trapped HSV-1 relative to the sample treated with no antibody, control (Figure 3.2, $p<0.05$ indicated by *). In contrast, HSV8 Agly and HSV8 Gal treated samples demonstrated significantly reduced trapping of HSV-1 relative to sample treated with HSV8 GnGn (Figure 3.2, $p<0.05$ indicated by *).

3.3 DISCUSSION

Specific terminal sugar residues on N-glycans of IgG-Fc can directly impact the Fc effector functions. For example, the absence of galactose increases inflammatory activity (Raju, 2008), whereas higher levels of galactose leads to enhanced complement dependent cytotoxicity (CDC) via increased binding to C1q (Raju, 2008). Galactose content does not appear to affect IgG binding to FcyRIIIa receptor, and hence possesses negligible influence on antibody-dependent cell mediated cytotoxicity (ADCC). On the other hand, IgG with terminal GlcNAc (N-acetyl-glucosamine), rather than galactose, exhibits increased binding to mannose, decreased serum half-life, as well as decreased CDC activity (Raju, 2008) The absence of terminal fucose leads to efficient binding to FcyRIII receptors and consequently enhanced ADCC activity. (Raju,

2008) Last but not least, increased sialic acid content has been correlated with increased anti-inflammatory activity, longer serum half-life, and decreased ADCC activity. (Raju, 2008, Wang et al., 2011, Ravetch et. al, 2010, and Kaneko, 2006)

In this chapter, I explored whether IgG glycosylation may impact IgG-mucin affinity – a largely under-recognized mechanism of mucosal immunity. In good agreement with the earlier observations of Fc- and N-glycan dependence, I found that subtle changes in N-glycan patterns on IgG-Fc can markedly alter IgG-mucin affinity, and consequently the potency with which Herpes-specific IgG immobilizes individual HSV-1 virions. Even a single sugar residue difference, from terminal galactose to terminal N-acetyl-glucosamine, substantially decreases the trapping potency. In contrast, terminal fucose did not appear to contribute to the interactions between IgG and mucins, as IgG containing the biantennary structure without terminal fucose (HSV8-GnGn) exhibited comparable potency as IgG with terminal fucose (HSV8-Human). The current known relationship between N-glycosylation and different IgG effector functions is summarized in Table 3.2. Unfortunately, due to unresolved technical challenges, I was unable to explore the impact of terminal sialic acid on IgG-mucin affinity at this time, and remains an important area open for future investigation.

Since galactose-rich IgG exhibits increased CDC activity, their poor trapping potency in mucus may seem counter-intuitive at first. However, in the absence of inflammation or infection, complement activity is typically low or even below detection levels in genital secretions from the healthy vagina (Cone, 1999; Hill and Anderson, 1992; Schumacher, 1988), and thus galactose-terminated IgG may not play an essential role in protective vaginal immunity against initial infections. The moderately reduced HSV-1 mobility observed with HSV8-Agly

suggests IgG-mucin interactions may extend beyond N-glycans, and that the amino acids of the Fc-domain may also participate in the associations with the mucin mesh.

Mucus specimens between different donors can vary substantially with age, diet, vaginal hygiene and sexual activity. Likewise, variations within the same donor can be attributed to menstrual cycle, diet, hydration, sexual activity and dynamic shifts in the vaginal microbiota.(Cone 1999) As is common with many studies involving mucus secretions, I observed substantial variations in pathogen mobility and trapping potency among different donor specimens. Hence, it will be necessary to substantially expand the current studies to make more definitive conclusions to the role of N-glycosylation on IgG-mucin affinity.

3.4 METHODS

3.4.1 Lectin Blot for Glycan Analysis

Around 5 ug of each of the antibodies were loaded onto a 4-12% Bis-Tris SDS gel and run under non-reducing conditions. The proteins were then transferred onto nitrocellulose membrane (run for 1.5 hours at 30V) using the X-cell blot system. The membrane was then rinsed briefly in PBS-Tween (0.01%) and then blocked with 1x carbo free blocking solution (Vector labs) for an hour at room temperature. Following this step, the membranes were briefly rinsed with PBS-Tween (PBST) and then one of the four different biotinylated lectins (4ug/ml) was added to each individual membrane and incubated overnight at 4 degrees celsius. Four different lectins were used to confirm the glycan profile of the antibodies, they are Con A (specificity to mannose), SNA (specificity to alpha 2,6 sialic acid), ECL (specificity to terminal galactose) and AAL (specificity to fucose). After the overnight incubation, the membrane was washed three times with PBST, 5 minutes per wash, and then secondary antibody, anti-biotin HRP, at a dilution of 1:30,000 was added to the membranes. After an hour of incubation at room temperature, the membranes were washed again, and incubated for 5 minutes with ECL reagent (BioRad). The membrane was patted down onto tissue paper to remove excess reagent and developed in a dark room using x-ray films. All the incubation steps were done while shaking.

3.4.2 Plantibodies

Plantibodies were generously donated by MAPP Pharmaceuticals who provided us with the chart characterizing the different glycoforms present in each antibody sample.

3.4.3 Cervicovaginal mucus (CVM) collection and characterization

CVM collection was performed as published previously (Lai et al., 2009a; Lai et al., 2010). Briefly, undiluted CVM secretions were obtained from women of reproductive age, by using a self-sampling menstrual collection device following protocols approved by the Institutional Review Board of the University of North Carolina – Chapel Hill. Informed consent of participants was obtained after the nature and possible consequences of the study were explained. The device was inserted into the vagina for at least 30 s, removed, and placed into a 50 mL centrifuge tube. Samples were centrifuged at 230 xg for 2 min to collect the secretions.

3.4.4 Multiple particle tracking of HSV-1 in CVM

To mimic neutralization of CVM by alkaline seminal fluid, we titrated CVM to pH 6.8-7.1 using small volumes (~3% v/v) of 3 N NaOH, and confirmed pH using a micro pH electrode (Microelectrodes, Inc., Bedford, NH) calibrated to pH 4, 7 and 10 buffers. Fluorescently tagged HSV-1 particles were incubated with Human HSV8, HSV8- GnGn, HSV8- Gal, HSV8- Agly or no Ab (Control) for an hour at room temperature. This mixture was then added to 20 μL of CVM placed in a custom-made glass chamber, and incubated for 1 hr at 37°C prior to microscopy. The translational motions of the particles were recorded using an EMCCD camera (Evolve 512; Photometrics, Tucson, AZ) mounted on an inverted epifluorescence microscope (AxioObserver D1; Zeiss, Thornwood, NY), equipped with an Alpha Plan-Apo 100x/1.46 NA objective, environmental (temperature and CO_2) control chamber and an LED light source (Lumencor Light Engine DAPI/GFP/543/623/690). Videos (512 x 512, 16-bit image depth) were captured with MetaMorph imaging software (Molecular Devices, Sunnyvale, CA) at a temporal resolution

of 66.7 ms and spatial resolution of 10 nm (nominal pixel resolution 0.156 μm/pixel) for 20 s. Particle trajectories were analyzed using IDL; Trapped particles were defined as those with effective diffusivity (D_{eff}) < 0.01 $\mu m^2/s$ at a time scale (τ) of 1 s (i.e., particles move less than their diameter within 1 s). Three independent experiments in CVM from different donors, with n ≥100 particles per experiment, were performed for each condition.

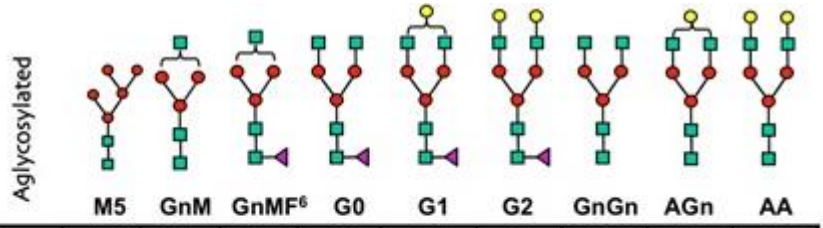

Rituxan					53	35		8		
h-13F6$_{GnGn}$	5		5					90		
h-13F6$_{Gal}$	5							20	23	45
h-13F6$_{agly}$	100									

Table 3.1: Summary of distribution of glycoforms present in the different plantibodies. The table was produced by MAPP pharmaceuticals, company that provided us with the plantibodies.

Terminal Sugar	CDC	ADCC	IgG-Mucin Affinity
GlcNAc	*Decrease*	*No effect*	*Increase*
Galactose	*Increase*	*No effect*	*Decrease*
Sialic Acid	*No effect*	*Decrease*	*TBD*
Fucose	*No effect*	*Decrease*	*No effect*

Table 3.2: Summary of how different terminal sugars affect antibody's immune function, especially CDC, ADCC activities as well as IgG-Mucin Affinity.

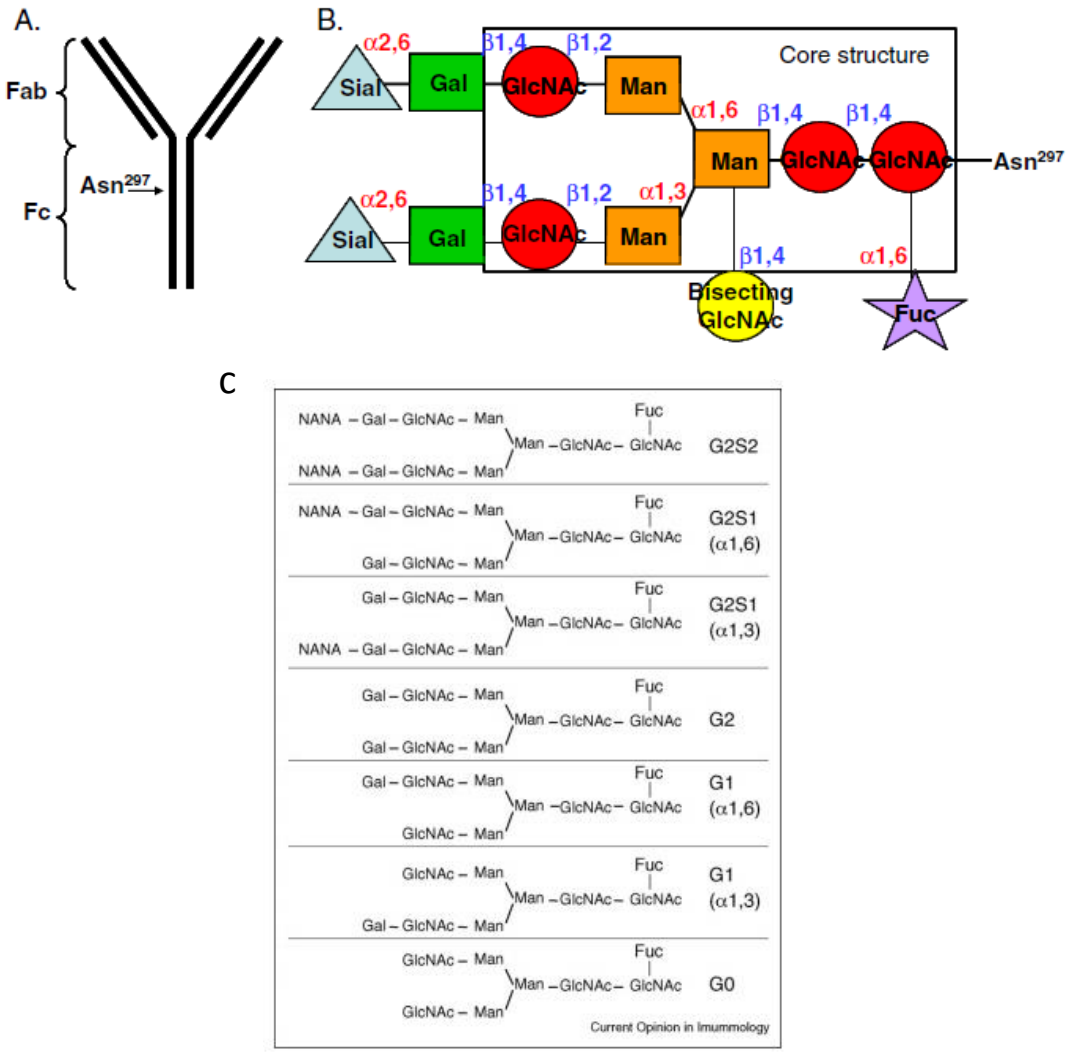

Figure 3.1: A. Glycans are present in the Asn 297 site of IgG. B. Schematic of N-linked glycan structure present in the Fc region. C. Structure of major N-glycans found in human IgG. The majority of glycans found in the Fc of human IgG are shown. These glycans are complex biantennary structures with heterogeneity because of terminal galactose and/or sialic acid residues (NANA, N-acetylneuraminic acid; Gal, galactose; GlcNAc, N-acetylglucosamine; Man, mannose; Fuc, fucose). About 10% of these glycans may not contain core Fucose residue (not shown) (Figure 3.1A and 3.1B from Anthony et al., 2010 and Figure 3.1C from Raju, 2008)

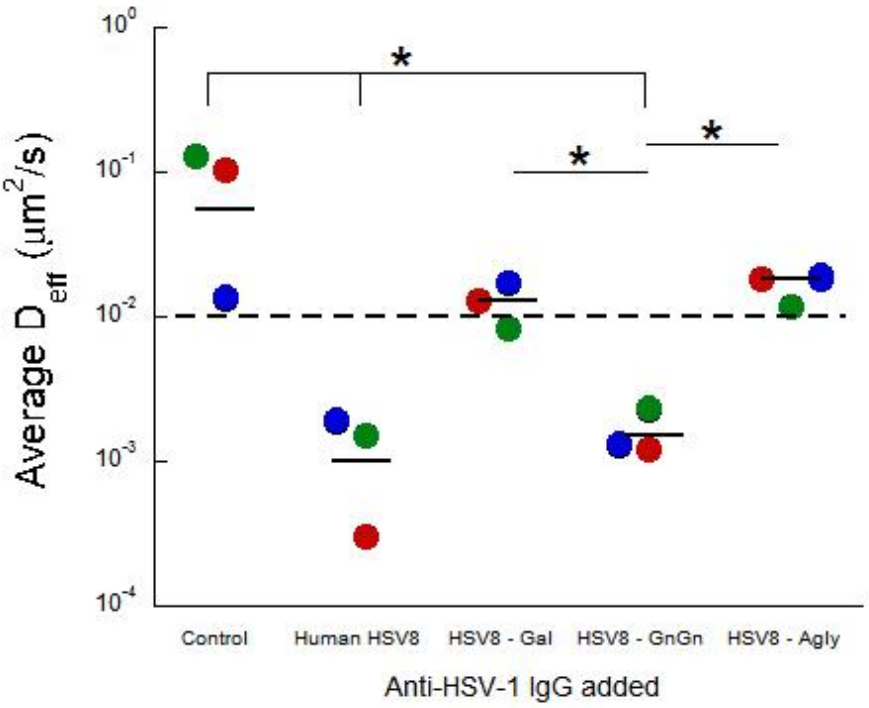

Figure 3.2: Mobility (Deff, t = 1s) of HSV-1 in CVM incubated with various HSV-1 specific Ab. Distinct samples (n=3, each experiment performed independently) are indicated with different color circles; geometric averages are indicated by solid lines. Dashed line represents the Deff cutoff below which particles are permanently trapped (moving less than their diameter within 1s). * indicates statistically significant difference ($p<0.05$) based off of one tailed distribution and two sample with equal variance ttest.

REFERENCES

- Anumula, K. R. (2012). Quantitative glycan profiling of normal human plasma derived immunoglobulin and its fragments fab and fc. Journal of Immunological Methods, 382, 167-176.
- Berzofsky, J.A., I.J. Berkower, and S.L. Epstein. 1993. Antigen-antibody interactions and monoclonal antibodies. *In* Fundamental Immunology. W.E. Paul, editor The Raven Press, New York, NY. 421-465.
- Clamp, J.R. 1977. The relationship between secretory immunoglobulin A and mucus [proceedings]. *Biochem. Soc. Trans.* 5:1579-1581.
- Cole, A.M. 2006. Innate host defense of human vaginal and cervical mucosae. *Curr. Top. Microbiol. Immunol.* 306:199-230.
- Cone, R.A. 1999. Mucus. *In* Handbook of Mucosal Immunology. P.L. Ogra, J. Mestecky, M.E. Lamm, W. Strober, J. Bienenstock, and J.R. McGhee, editors. Academic Press, San Diego, CA. 43-64.
- Cone, R.A., T. Hoen, X. Wong, R. Abusuwwa, D.J. Anderson, and T.R. Moench. 2006. Vaginal microbicides: detecting toxicities in vivo that paradoxically increase pathogen transmission. *BMC Infect. Dis.* 6:90.
- Crowther, R., S. Lichtman, J. Forstner, and G. Forstner. 1985. Failure to show secretory IgA binding by rat intestinal mucin. *Fed. Proc.* 44:691.
- Crowther, R.S., and R.F. Wetmore. 1987. Fluorometric assay of O-linked glycoproteins by reaction with 2-cyanoacetamide. *Anal. Biochem.* 163:170-174.
- Dalziel, M., McFarlane, I., & Axford, J. S. (1999). Lectin analysis of human immunoglobulin g n-glycan sialylation. Glycoconjugates Journal, 12, 801-807.
- De Logu, A., Williamson, R., Rozenshteyn, R., Ramiro-Ibanez, F., Simpson, C. D., Burton, D. R., & Sanna, P. (1998). Characterization of a type-common human recombinant monoclonal antibody to herpes simplex virus with high therapeutic potential. Journal of Clinical Microbiology, 36(11), 3198-3204.
- Doss, M., M.R. White, T. Tecle, and K.L. Hartshorn. 2010. Human defensins and LL-37 in mucosal immunity. *J. Leukoc. Biol.* 87:79-92.
- Elliott, G., and P. O'Hare. 1999. Live-cell analysis of a green fluorescent protein-tagged herpes simplex virus infection. *J. Virol.* 73:4110-4119.
- Ha, S., Y. Ou, J. Vlasak, Y. Li, S. Wang, K. Vo, Y. Du, A. Mach, Y. Fang, and N. Zhang. 2011. Isolation and characterization of IgG1 with asymmetrical Fc glycosylation. *Glycobiology* 21:1087-1096.
- Hamburger, A.E., P.J. Bjorkman, and A.B. Herr. 2006. Structural insights into antibody-mediated mucosal immunity. *Curr. Top. Microbiol. Immunol.* 308:173-204.
- Heine, J.W., R.W. Honess, E. Cassai, and B. Roizman. 1974. Proteins specified by herpes simplex virus. XII. The virion polypeptides of type 1 strains. *J. Virol.* 14:640-651.

- Hill, J.A., and D.J. Anderson. 1992. Human vaginal leukocytes and the effects of vaginal fluid on lymphocyte and macrophage defense functions. *Am J Obstet Gynecol* 166:720-726.
- Huhn, C., Selman, M., Renee Ruhaak, L., Deelder, A.M., and Wuhrer, M. 2009. IgG glycosylation analysis. *Proteomics*, 9, 882-913
- Jager, S., J. Kremer, J. Kuiken, and I. Mulder. 1981. The significance of the Fc part of antispermatozoal antibodies for the shaking phenomenon in the sperm-cervical mucus contact test. *Fertil. Steril.* 36:792-797.
- Kaneko, Y., Nimmerjahn, F., & Ravetch, J. (2006). Anti-inflammatory activity of immunoglobulin g resulting from fc sialylation. Science, 313, 670-673.
- Kobayashi, K., H. Ogata, M. Morikawa, S. Iijima, N. Harada, T. Yoshida, W.R. Brown, N. Inoue, Y. Hamada, H. Ishii, M. Watanabe, and T. Hibi. 2002. Distribution and partial characterisation of IgG Fc binding protein in various mucin producing cells and body fluids. *Gut* 51:169-176.
- Kocevar-Nared, J., J. Kristl, and J. Smid-Korbar. 1997. Comparative rheological investigation of crude gastric mucin and natural gastric mucus. *Biomaterials* 18:677-681.
- Kremer, J., and S. Jager. 1976. The sperm-cervical mucus contact test: a preliminary report. *Fertil. Steril.* 27:335-340.
- Kresge, K.J. 2009. The Mysteries of Protection. *IAVI Report Vol 13, Number 5*
- Kresge, K.J. 2011. A Bangkok Surprise. *IAVI Report Vol 15, Number 5*
- Lai, S.K., K. Hida, S. Shukair, Y.Y. Wang, A. Figueiredo, R. Cone, T.J. Hope, and J. Hanes. 2009a. Human immunodeficiency virus type 1 is trapped by acidic but not by neutralized human cervicovaginal mucus. *J. Virol.* 83:11196-11200.
- Lai, S.K., D.E. O'Hanlon, S. Harrold, S.T. Man, Y.Y. Wang, R. Cone, and J. Hanes. 2007. Rapid transport of large polymeric nanoparticles in fresh undiluted human mucus. *Proc. Natl. Acad. Sci. U.S.A.* 104:1482-1487.
- Lai, S.K., Y.Y. Wang, D. Wirtz, J. Hanes. 2009. Micro- and macrorheology of mucus. Advanced Drug Delivery Reviews. 61:86-100.
- Lai, S.K., Y.Y. Wang, and J. Hanes. 2009b. Mucus-penetrating nanoparticles for drug and gene delivery to mucosal tissues. *Adv. Drug Deliv. Rev.* 61:158-171.
- Lai, S.K., Y.Y. Wang, K. Hida, R. Cone, and J. Hanes. 2010. Nanoparticles reveal that human cervicovaginal mucus is riddled with pores larger than viruses. *Proc. Natl. Acad. Sci. U.S.A.* 107:598-603.
- Li, Z., S. Palaniyandi, R. Zeng, W. Tuo, D.C. Roopenian, and X. Zhu. 2011. Transfer of IgG in the female genital tract by MHC class I-related neonatal Fc receptor (FcRn) confers protective immunity to vaginal infection. *Proc. Natl. Acad. Sci. U.S.A.* 108:4388-4393.

- Mantis, N.J., N. Rol, and B. Corthesy. 2011. Secretory IgA's complex roles in immunity and mucosal homeostasis in the gut. *Mucosal Immunol.* 4:603-611.
- Mascola, J.R., G. Stiegler, T.C. VanCott, H. Katinger, C.B. Carpenter, C.E. Hanson, H. Beary, D. Hayes, S.S. Frankel, D.L. Birx, and M.G. Lewis. 2000. Protection of macaques against vaginal transmission of a pathogenic HIV-1/SIV chimeric virus by passive infusion of neutralizing antibodies. *Nature Med.* 6:207-210.
- Meysick, K.C., and G.E. Garber. 1992. Interactions between Trichomonas vaginalis and vaginal flora in a mouse model. *J. Parasitol.* 78:157-160.
- Nugent, R.P., M.A. Krohn, and S.L. Hillier. 1991. Reliability of diagnosing bacterial vaginosis is improved by a standardized method of gram stain interpretation. *J. Clin. Microbiol.* 29:297-301.
- Olmsted, S.S., J.L. Padgett, A.I. Yudin, K.J. Whaley, T.R. Moench, and R.A. Cone. 2001. Diffusion of macromolecules and virus-like particles in human cervical mucus. *Biophys. J.* 81:1930-1937.
- Phalipon, A., A. Cardona, J.P. Kraehenbuhl, L. Edelman, P.J. Sansonetti, and B. Corthesy. 2002. Secretory component: a new role in secretory IgA-mediated immune exclusion in vivo. *Immunity* 17:107-115.
- Raju, S. 2008. Terminal sugars of Fc glycans influence antibody effector functions of IgGs. *Current Opinion in Immunology*, 20, 471-478.
- Ravetch, J. V., & Anthony, R. M. (2010). A novel role for the igg fc glycan: The anti-inflammatory activity of sialylated igg fcs. Journal of Clinical Immunology, 30, 9-14.
- Rerks-Ngarm, S., P. Pitisuttithum, S. Nitayaphan, J. Kaewkungwal, J. Chiu, R. Paris, N. Premsri, C. Namwat, M. de Souza, E. Adams, M. Benenson, S. Gurunathan, J. Tartaglia, J.G. McNeil, D.P. Francis, D. Stablein, D.L. Birx, S. Chunsuttiwat, C. Khamboonruang, P. Thongcharoen, M.L. Robb, N.L. Michael, P. Kunasol, and J.H. Kim. 2009. Vaccination with ALVAC and AIDSVAX to prevent HIV-1 infection in Thailand. *N. Engl. J. Med.* 361:2209-2220.
- Saltzman, W.M., M.L. Radomsky, K.J. Whaley, and R.A. Cone. 1994. Antibody diffusion in human cervical mucus. *Biophys. J.* 66:508-515.
- Schumacher, G.F. 1988. Immunology of spermatozoa and cervical mucus. *Hum. Reprod.* 3:289-300.
- Usala, S.J., F.O. Usala, R. Haciski, J.A. Holt, and G.F. Schumacher. 1989. IgG and IgA content of vaginal fluid during the menstrual cycle. *J. Reprod. Med.* 34:292-294.
- Wang,J.,Balog, C., Stavenhagen, K., Koeleman, C., Scherer, H., Selman, Wuhrer, M. 2011. Fc-glycosylation of IgG1 is modulated by B-cell stimuli. *Molecular and Cellular Proteomics*, 10 1-12.
- Zeitlin, L., K.J. Whaley, T.A. Hegarty, T.R. Moench, and R.A. Cone. 1997. Tests of vaginal microbicides in the mouse genital herpes model. *Contraception* 56:329-335.